






High N6-methyladenosine-activated TCEAL8 mRNA is a novel pancreatic cancer marker

Tomoaki Hara¹ | Sikun Meng¹ | Hiromichi Sato^{1,2} | Shotaro Tatekawa³ | Kazuki Sasaki^{1,2} | Yu Takeda^{1,2}  | Yoshiko Tsuji¹ | Yasuko Arao¹ | Ken Ofusa^{1,4} | Toru Kitagawa^{1,2,5} | Daisaku Yamada²  | Hidenori Takahashi²  | Shogo Kobayashi² | Daisuke Motooka⁶ | Yutaka Suzuki⁷ | Sarah Rennie⁸ | Shizuka Uchida⁹ | Masaki Mori¹⁰ | Kazuhiko Ogawa³ | Yuichiro Doki² | Hidetoshi Eguchi²  | Hideshi Ishii¹ 

¹Department of Medical Data Science, Center of Medical Innovation and Translational Research, Osaka University Graduate School of Medicine, Suita, Osaka, Japan

²Department of Gastroenterological Surgery, Osaka University Graduate School of Medicine, Suita, Osaka, Japan

³Department of Radiation Oncology, Osaka University Graduate School of Medicine, Suita, Osaka, Japan

⁴Prophoenix Division, Food and Life-Science Laboratory, IDEA Consultants, Inc., Osaka, Osaka, Japan

⁵Kyowa-kai Medical Corporation, Kawanishi, Hyogo, Japan

⁶Genome Information Research Center, Research Institute for Microbial Diseases, Osaka University, Suita, Osaka, Japan

⁷Laboratory of Systems Genomics, Department of Computational Biology and Medical Sciences, Graduate School of Frontier Sciences, The University of Tokyo, Kashiwa-shi, Chiba, Japan

⁸Section for Computational and RNA Biology, Department of Biology, University of Copenhagen, Copenhagen, Denmark

⁹Department of Clinical Medicine, Center for RNA Medicine, Aalborg University, Copenhagen SV, Denmark

¹⁰Tokai University Graduate School of Medicine, Isehara, Kanagawa, Japan

Correspondence

Hidetoshi Eguchi, Department of Gastroenterological Surgery, Osaka University Graduate School of Medicine, Yamadaoka 2-2, Suita, Osaka 565-0871, Japan.

Email: heguchi@gesurg.med.osaka-u.ac.jp

Hideshi Ishii, Department of Medical Data Science, Center of Medical Innovation and Translational Research, Osaka University Graduate School of Medicine, Yamadaoka 2-2, Suita, Osaka 565-0871, Japan.

Email: hishii@gesurg.med.osaka-u.ac.jp

Funding information

Takahashi Industrial and Economic Research Foundation, Grant/Award Number: 2023; Mitsubishi Foundation,

Abstract

N6-methyladenosine (m6A) is an RNA modification involved in RNA processing and widely found in transcripts. In cancer cells, m6A is upregulated, contributing to their malignant transformation. In this study, we analyzed gene expression and m6A modification in cancer tissues, ducts, and acinar cells derived from pancreatic cancer patients using MeRIP-seq. We found that dozens of RNAs highly modified by m6A were detected in cancer tissues compared with ducts and acinar cells. Among them, the m6A-activated mRNA TCEAL8 was observed, for the first time, as a potential marker gene in pancreatic cancer. Spatially resolved transcriptomic analysis showed that TCEAL8 was highly expressed in specific cells, and activation of cancer-related signaling pathways was observed relative to TCEAL8-negative

Abbreviations: GEO, Gene Expression Omnibus; IGV, Integrative Genomics Viewer; m6A, N6-methyladenosine; MeRIP-seq, methylated RNA immunoprecipitation sequencing; scRNA-seq, single-cell RNA-seq; TCGA, The Cancer Genome Atlas.

Tomoaki Hara and Sikun Meng contributed equally to this work.

This is an open access article under the terms of the [Creative Commons Attribution-NonCommercial-NoDerivs](https://creativecommons.org/licenses/by-nc-nd/4.0/) License, which permits use and distribution in any medium, provided the original work is properly cited, the use is non-commercial and no modifications or adaptations are made.

© 2024 The Authors. *Cancer Science* published by John Wiley & Sons Australia, Ltd on behalf of Japanese Cancer Association.

Grant/Award Number: 2021-48; Japan Science and Technology Agency, Grant/Award Number: 17cm0106414h0002; JP21lm0203007; JP23ym0126809; 19K22658; 20H00541; 21K19526; 22H03146 and 22K19559; 16H06279 (PAGS)

cells. Furthermore, among TCEAL8-positive cells, the cells expressing the m6A-modifying enzyme gene METTL3 showed co-activation of Notch and mTOR signaling, also known to be involved in cancer metastasis. Overall, these results suggest that m6A-activated TCEAL8 is a novel marker gene involved in the malignant transformation of pancreatic cancer.

KEYWORDS

m6A, MeRIP-seq, METTL3, pancreatic cancer, TCEAL8

1 | INTRODUCTION

N6-methyladenosine (m6A) is a modified RNA with a methyl group attached to the amino group of adenine.¹ Many RNAs, including rRNA, U6 snRNA, mRNA, and ncRNA, undergo post-transcriptional m6A functional modification in cells, and m6A modification is involved in the regulation of their functions and gene expression.^{2–4} METTL3 has been identified as a representative m6A-modifying enzyme and has been found to modify the central adenine of its binding sequence, RRACH (R: A or G, H: A, T, or C).⁵ The enzyme that performs the m6A modification is defined as a writer, the protein that binds to the m6A modification site is defined as a reader, and the enzyme that removes the m6A modification is defined as an eraser.⁶ METTL3, which modifies mRNA, ZC6Hc4, which modifies 28S rRNA, and METTL16, which modifies U6 snRNA, have been identified as writers.⁷ IGF2BP family, YTHDC1, and YTHDF family have been identified as readers, and FTO and ALKBH5 have been identified as erasers.⁸

Methylated RNA immunoprecipitation sequencing (MeRIP-seq) uses m6A antibodies to collect and sequence m6A-containing RNA from total RNA extracted from cells, thereby identifying m6A-activated sites.⁹ MeRIP-seq has been performed on various cancer cell tumors, and m6A has been found to be associated with malignant transformation of cancer.¹⁰ It has been reported that inhibition of expression of METTL14 (m6A methyltransferase) and ALKBH5 (demethylase) in human breast cancer cell lines inhibits cancer growth and invasion.¹¹ The 3' UTR of homeobox containing 1 (HMBX1) mRNA is modified with m6A by METTL3, and its translation is repressed in prostate cancer cell LNCaP compared with epithelial cell RWPE-1, a normal cell line, and telomere length and p53 signaling are aberrant.¹² In pancreatic cancer, m6A of polo-like kinase 1 (PLK1) mRNA modified by METTL3 has been reported to be essential for the cell cycle.¹³ LINC00662 m6A activates focal adhesion through the GTF2B-ITGA1-FAK pathway and is involved in malignant transformation of pancreatic cancer.¹⁴ Modification of LINC00941 with m6A is also promoted by METTL14, and binding of IGF2BP2 stabilizes LINC00941 and promotes migration and invasion.¹⁵ Thus, highly m6A-modified RNAs are involved in malignant transformation of cancers and expected to become targets for diagnosis and therapy as cancer cell markers. To improve the accuracy of these medical technologies, knowledge of the m6A modification status of cancer tissue and surrounding normal tissue is needed. In this study, we identify pancreatic cancer tissue-specific m6A hypermodified gene markers by comparing gene expression and m6A-modified genes between pancreatic cancer clinical samples and normal tissue cells.

2 | MATERIALS AND METHODS

2.1 | Human samples

The cancer, duct, and acinar tissues used in this study were surgically resected samples from human pancreatic cancer patients. MeRIP-seq used tissues obtained from a total of four pancreatic cancer patients, three males and one female. The average age of the patients was 67 years old, and they had stage 2 pancreatic cancer. The Visium analysis used samples derived from an 81-year-old stage 1 male pancreatic cancer patient. The study was approved by the Ethical Review Committee of Osaka University and was conducted in accordance with the regulations.

2.2 | RNA extraction

Surgical samples from patients were cut into reasonable sizes, placed on RNeasy (Sigma-Aldrich), and stored at -80°C . Organoids were prepared by PancreaCult™ organoid media (Human) (STEMCELL Technologies) from one patient sample. The tissue was cut into small pieces and treated with accutase (Innovative Cell Technologies, Inc.) The tissue was then mixed with Matrigel (Corning) and spread on 24-well plates. After incubation with organoid initiation medium (OIM) (5% PancreaCult™ organoid growth supplement [Human], 10% organoid supplement, 50 ng/μL EGF, 1 μM PGE2, and 10 μM Y-27632) in a CO₂ incubator at 37°C for 3 days, the organoid was cultured in organoid growth medium (OGM) (OIM composition minus organoid supplement and Y-27632) in a CO₂ incubator at 37°C. After four patient samples were collected, samples were crushed and RNA was extracted by ISOGEN (NIPPON GENE). Then, 0.2 mL of chloroform was added to mixture of crushed tissue samples and 1 mL of ISOGEN. After mixing and centrifuge, the aqueous layer was collected and RNA was recovered by isopropanol precipitation.

2.3 | MeRIP-seq

Extracted RNA was mixed with a final concentration of 100 mM Tris-HCl (pH 7.4) and 100 mM ZnCl₂ solution and incubated at 90°C for 2 min to fragment to a reasonable length. Then, 0.5 M EDTA was added to stop fragmentation. Ethanol precipitation

was performed, and the recovered RNA was used for RNA-seq as input RNA. The input RNA was incubated in a final concentration of 10 mM Tris-HCl (pH 7.4), 150 mM NaCl, 0.1% IGEPAL CA-630 (Sigma-Aldrich), 1 μ L RNasin Plus RNase inhibitor 2500 (Promega), 2.5 μ L ribonucleoside vanadyl complexes (RVC) (Sigma-Aldrich), and 5 μ g anti-m6A rabbit polyclonal antibody (Synaptic Systems) and incubated at 4°C overnight to bind m6A and anti-m6A rabbit polyclonal antibody. Dynabeads Protein G for immunoprecipitation (Thermo Fisher scientific) was washed with the same buffer (except input RNA and m6A antibody, defined as wash buffer), added to the input RNA solution, and incubated at 4°C overnight to collect m6A RNA. After recovery of m6A RNA and m6A antibody complex by magnetic tube stand, the beads were washed with wash buffer and added to the elution buffer (final concentration of 6.7 mM N6-methyladenosine 5-monophosphate sodium salt [Sigma-Aldrich], 10 mM Tris-HCl [pH 7.4], 150 mM NaCl, 0.1% IGEPAL CA-630 [Sigma-Aldrich], 1 μ L RNasin Plus RNase inhibitor 2500 [Promega]). After vortex, beads were incubated at 4°C overnight to elute m6A RNA to anti-m6A antibodies. Supernatant containing m6A RNA was collected and ethanol precipitation was performed. Then RNA immunoprecipitation (RIP) RNAs were obtained and used in RNA-seq.

2.4 | RNA-seq

Input RNA and RIP RNA were sent to the University of Tokyo Center for Frontier Sciences, one of the Integrated Information Analysis Groups of the Platform for Advanced Genome Science, for RNA-seq. After sequencing with NovaSeq (S1), trimming was performed with fastp,¹⁶ and removal of ribosomal RNA with bowtie2¹⁷ and mapping with STAR were carried out.¹⁸ Bam files were read by Integrative Genomics Viewer (IGV)¹⁹ to confirm the mapping results. The obtained Fragments Per Kilobase of exon per Million mapped reads data were used for heat mapping and t-SNE plots using iDEP96²⁰ and for Volcano plots and identification of expression variation genes using BioJupies.²¹ KEGG²² pathway analysis was performed on cancer tissues using acinar cells and ducts as controls in Gene Set Enrichment Analysis (GSEA) software.²³

2.5 | Gene expression analysis using the pancreatic cancer database

A previously constructed pancreatic cancer database file (pk_all.rds) was used.²⁴ The data were read by R, and the expression of each gene was confirmed by Seurat's featureplot.²⁵ In Figure S5, Malignant_cell_clusters.rds, which is data for Ductal cell type2, was used to extract cells with TCEAL8 expression greater than 0. After that, the gene expression data were output and subjected to GSEA, with cells with METTL3 expression greater than 1 being METTL3-high-expressing cells and cells with METTL3 expression greater than 0 and less than 0.3 being METTL3-low-expressing cells.

2.6 | Spatially resolved transcriptomic (Visium) analysis

Patient-derived cancer and duct tissue sections were sent to the University of Tokyo Center for Frontier Sciences, one of the Integrated Information Analysis Groups of the Platform for Advanced Genome Science, for spatially resolved transcriptomic analysis. Sequencing was performed with NovaSeq (SP), and loupe files were obtained using Space Ranger (10x GENOMICS). Space Ranger output files were read by Seurat in R, expression data were exported, and GSEA was performed.

2.7 | Statistical analysis

The *p*-values were calculated by BioJupies or GSEA software.

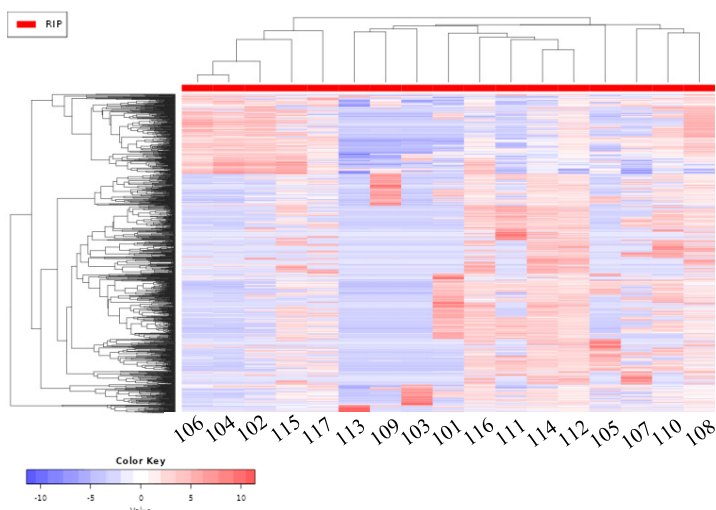
3 | RESULTS

3.1 | Pancreatic cancer tissue has higher m6A-activated RNA than normal tissue

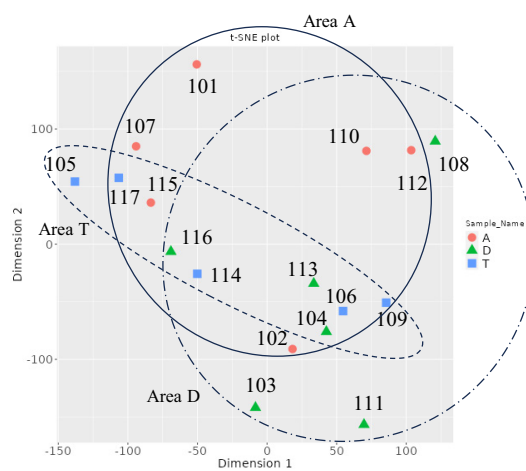
To identify pancreatic cancer tissue-specific m6A-activated RNAs, pancreatic cancer tissue and surrounding ducts and acinar cells derived from four patients were collected. For one patient, the tissue was divided into two parts, collecting a total of five samples from each, and total RNA was extracted from each tissue. One patient's duct and acinar cells were cultured to grow organoids, and total RNA was also extracted from the organoids. MeRIP was then performed to identify m6A-modified RNA in these total RNAs, and RNA-seq was performed on the RNA after recovery (RIP RNA) and before addition of m6A antibody (input RNA). Differences were observed in genes with variable expression between each sample (Figure 1A, Figure S1A). When the gene expression of each sample was dimensionally compressed and plotted in a t-SNE plot, the cancer tissue was located in a wider region in the input RNA as well as in the ductal and acinar cells, but in the RNA samples after MeRIP it was located in a narrower region compared with the ductal and acinar cells (Figure 1B, Figure S1B). These results suggest that there may be some pattern in the m6A-modified state of the RNA, although gene expression in each tissue may differ significantly in each patient.

When we examined genes specifically expressed in cancer tissues compared with duct and acinar cells, we detected insulin (INS), Trefoil Factor 1 (TFF1), and zinc finger C2HC-type containing 1B (ZC2HC1B) as genes with log2FC values greater than 4 in RIP RNA and SNORD80 and SNORD112 as genes with log2FC values greater than 5 in input RNA (Figure 1C, Figure S1C). The top 20 genes had log2FC values above 3 in both RIP RNA and input RNA (Figure 1D, Figure S1D). In RIP RNA, RMDN2-AS1, transcription elongation factor A-like 8 (TCEAL8), and APCDD1L-AS1, which have rarely been reported as cancer markers, were detected as genes modified highly with m6A (Figure 1D). In input RNA, small nucleolar RNA, C/D box

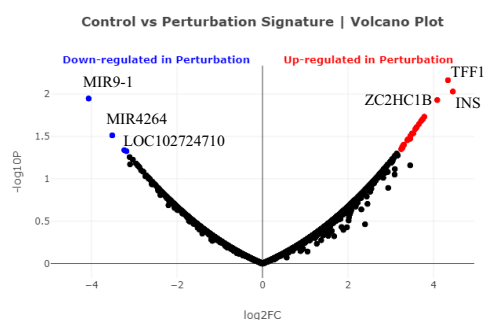
(A)



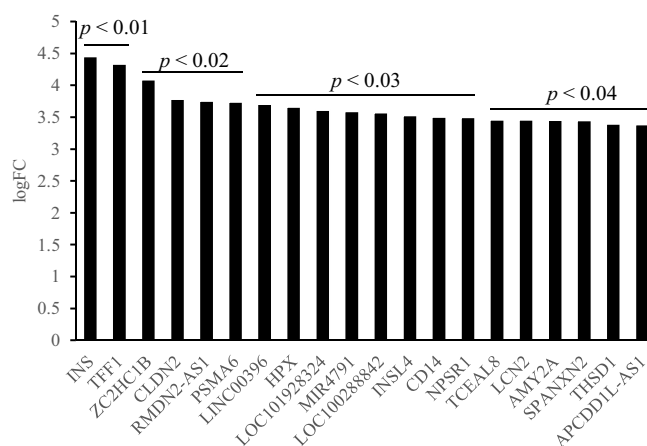
(B)



(C)



(D)



(E)

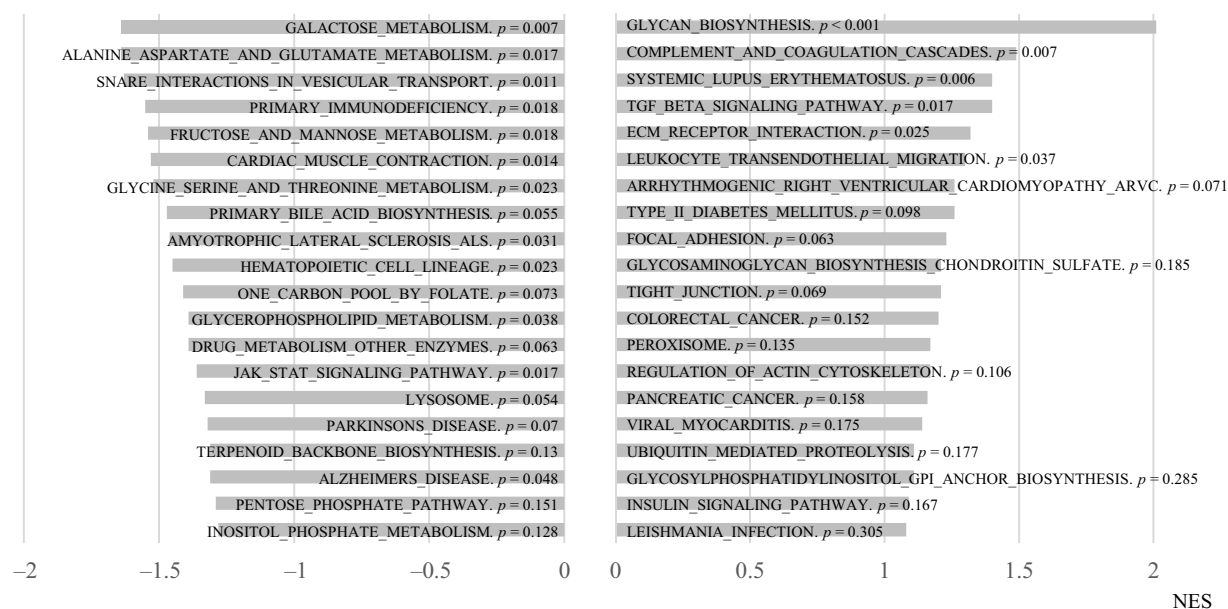


FIGURE 1 Results of methylated RNA immunoprecipitation sequencing (MeRIP-seq). (A) Heat map of the top 1000 variable genes. (B) Gene expression of each sample is dimensionally compressed and represented in t-SNE plot. 101, 102, 107, 112, and 115 are acinar cells; 103, 104, 108, 113, and 116 are ductal tissue; 105, 106, 109, 114, and 117 are cancer tissue; 110 is acinar cell organoid derived from 107; 111 is duct cell organoids derived from 108. (C) Volcano plot of genes with variable expression in cancer tissues, with acinar and ductal tissues as controls. (D) Top 20 genes upregulated in (C). (E) GSEA of cancer tissues using KEGG pathway, with the acinar and ductal tissues as controls. Horizontal axis is normalized enrichment score (NES).

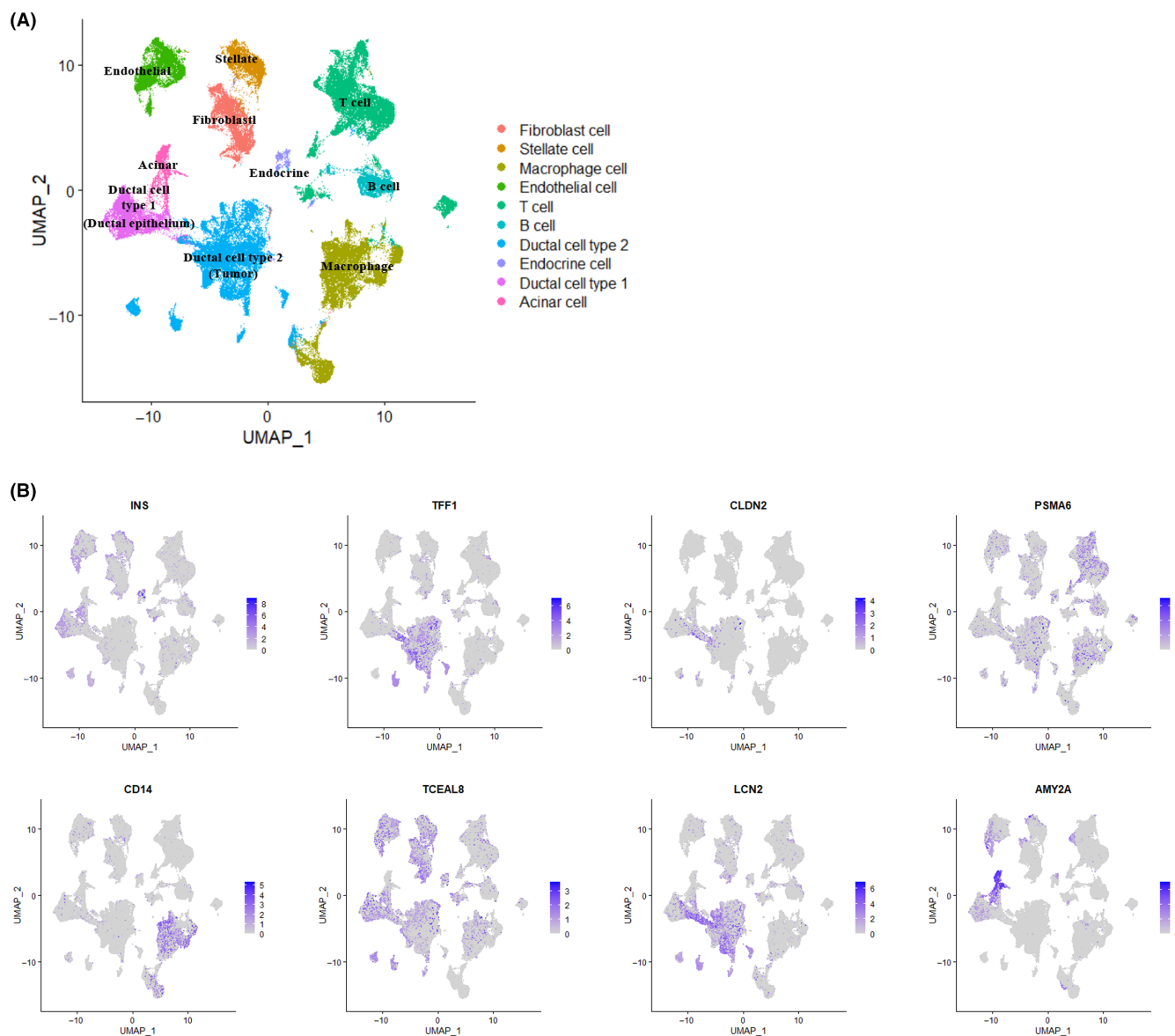


FIGURE 2 Gene expression results for each gene from the pancreatic cancer single-cell analysis database. (A) Two-dimensional illustration of each cell type by Umap. The pk_all.rds file reported previously was used. (B) Gene expression distribution of INS, TFF1, CLDN2, PSMA6, CD14, TCEAL8, LCN2, and AMY2A.

(SNORD) and small nucleolar RNA, H/ACA box (SNORA) family genes accounted for half of the top 20 genes (Figure S1D). KEGG pathway analysis of RIP RNA using GSEA in normal tissue ducts and acinar cells as controls revealed that pancreatic cancer-related pathways and the TGF β signaling pathway were detected as activated pathways in cancer tissues and that sugar metabolism such as galactose and amino acid metabolism such as alanine, aspartic acid, and

glutamic acid were detected as inactivated pathways (Figure 1E). This result suggests that pathways involved in cell proliferation are highly m6A activated in cancer tissues, while genes involved in sugar and amino acid metabolism are low m6A activated. In input RNA, KEGG pathway analysis of cancer tissue using normal tissue ducts and acinar cells as controls detected pancreatic cancer-related pathways and TGF β signaling pathways as activated pathways, while the

amino acid metabolism such as alanine, aspartate, and glutamate, Hedgehog, and PPAR pathways were detected as inactivated pathways (Figure S1E). These results suggest that m6A modification and gene expression levels are positively correlated.

3.2 | m6A-activated RNAs are likely to be highly expressed from specific cell types

To determine the types of cells in which cancer tissue-specific genes detected by MeRIP are expressed, we used the pancreatic cancer single-cell RNA-seq (scRNA-seq) data (Pancreatic Cancer Atlas) that we constructed by integrating data previously available on GEO (PRJCA001063, GSE111672, GSE154778, GSE155698, and GSM4293555) and our own sample data²⁴ (Figure 2A). Expression levels of the genes obtained in Figure 1D were examined on the Pancreatic Cancer Atlas, and high-expressing cells were detected in INS, TFF1, claudin 2 (CLDN2), proteasome 20S subunit alpha 6 (PSMA6), CD14, TCEAL8, lipocalin 2 (LCN2), and amylase alpha 2A (AMY2A) (Figure 2B). INS was mainly expressed in acinar cells, endocrine cells, and endothelial cells; TFF1 was expressed in ductal cell type 2, which is cancer cells; CLDN2 was expressed in ductal cell type 1 and ductal cell type 2; PSMA6 was expressed in all cell types, but mainly in T cells; CD14 in macrophages; TCEAL8 in various cell types, but mainly in fibroblast and surrounding cells including cancer cells (ductal cell type 2); LCN2 in ductal cell type 2; and AMY2A in acinar cells (Figure 2B). These results suggest that the highly m6A-modified RNA may be originated from the specific cell types.

3.3 | Coding sequence (CDS) of TCEAL8 mRNA is highly modified with m6A in pancreatic cancer tissue

Since TCEAL8, one of the highly m6A-modified mRNA detected in MeRIP-seq, has not been reported to have much to do with cancer, we decided to focus on TCEAL8 and investigate its function. We searched for METTL3-binding sequences (RRACH) in TCEAL8 mRNA to determine which adenines are hypermethylated. We found 16 binding sequences in the TCEAL8 genomic DNA sequence, zero for exon 1 and exon 2, seven in the protein coding sequence (CDS) of exon 3, and nine RRACH sequences distributed in the 3' untranslated region (3' UTR) of exon 3 (Figure 3A). To determine which of these METTL3-binding sequences were highly m6A modified, we referred to the mapping of RNA-seq-derived sequence data to the genome (Figure 3B,C, Figure S2A,B). The RIP117 cancer tissue showed a more remarkable mapping to the CDS region of exon 3 than the RIP115 acinar cells or the RIP116 ducts (Figure 3B). Another patient-derived sample, RIP114 cancer tissue, also showed exon 3 mapping compared with RIP112 acinar cells and RIP113 ducts (Figure 3C). TCEAL8 mRNA mapping of the other two patient-derived samples also showed that there were fewer counts in the RIP109 cancer tissue compared with the RIP107 acinar cells and RIP108 ducts (Figure S2A), although RIP105 and RIP106 cancer

tissues showed counts that were higher than those of RIP101 acinar cells, RIP103 ducts, and RIP104 ducts, except for RIP102 acinar cells (Figure S2B). There was little mapping in RIP110 organoid culture-derived acinar cells and RIP111 organoid culture-derived ducts (Figure S2A). These results suggest that the CDS region of exon 3 is more likely to be a m6A modification in cancer tissues compared with normal acinar cells and ducts, although the degree of TCEAL8 m6A modification varies in each patient. In addition, the 3' UTR was low count, suggesting that among the RRACH sequences in the CDS region, AAACA, AAACC, and GAACA sequences, which are also present in the 3' UTR, are low m6A, and GGACA, GGACC, and AGACA are high m6A (Figure 3A).

3.4 | Gene expression is upregulated or downregulated by m6A

To determine how m6A affects gene expression, we examined changes in gene expression for high m6A-activated genes in cancer cells. The expression of many genes was increased by m6A modification, but some genes' expression was decreased (Figure S3A,B). This suggests that the m6A modification affects both up- and downregulation of gene expression. To identify other m6A markers, we compared the RIP of cancer cells with the inputs of ductal and acinar cells. Many genes with LogFC greater than 3 were detected (Figure S3C). This suggests that m6A-modified mRNAs of these genes may be pancreatic cancer markers. Two-dimensional plots of RIP and input gene expression levels for TCEAL8 in individual patients showed a positive correlation between them, suggesting that m6A modification of TCEAL8 mRNA upregulates TCEAL8 expression (Figure S4A). Regarding the RIP of TCEAL8, the expression level of m6A-activated TCEAL8 mRNA was higher in tumors than in ducts, suggesting that m6A-activated TCEAL8 mRNA is cancer specific (Figure S4B). Activation of splicing-related factors and Notch signaling pathways was observed in METTL3-high-expressing cells for TCEAL8-positive cells in cancer single-cell data (Figure S5).

3.5 | TCEAL8 is expressed in specific regions of pancreatic cancer tissues

A spatially resolved transcriptomic (Visium) analysis was performed on cancer tissue to determine the distribution of TCEAL8-expressing cells. Gene expression data were obtained from 2623 spots on cancer tissue sections. TCEAL8 was detected in 332 spots and distributed over a wide area of cancer tissue (Figure 4A). We decided to compare gene expression in TCEAL8-positive and TCEAL8-negative spots to determine what function TCEAL8 may have. GSEA using gene expression data from 2607 spots after quality check revealed activation of cancer-related signals in TCEAL8-positive spots compared with TCEAL8-negative spots (Figure 4B). To confirm the effect of the number of genes detected in each spot on the analysis, the 26 spots with less than 500 genes detected were excluded and

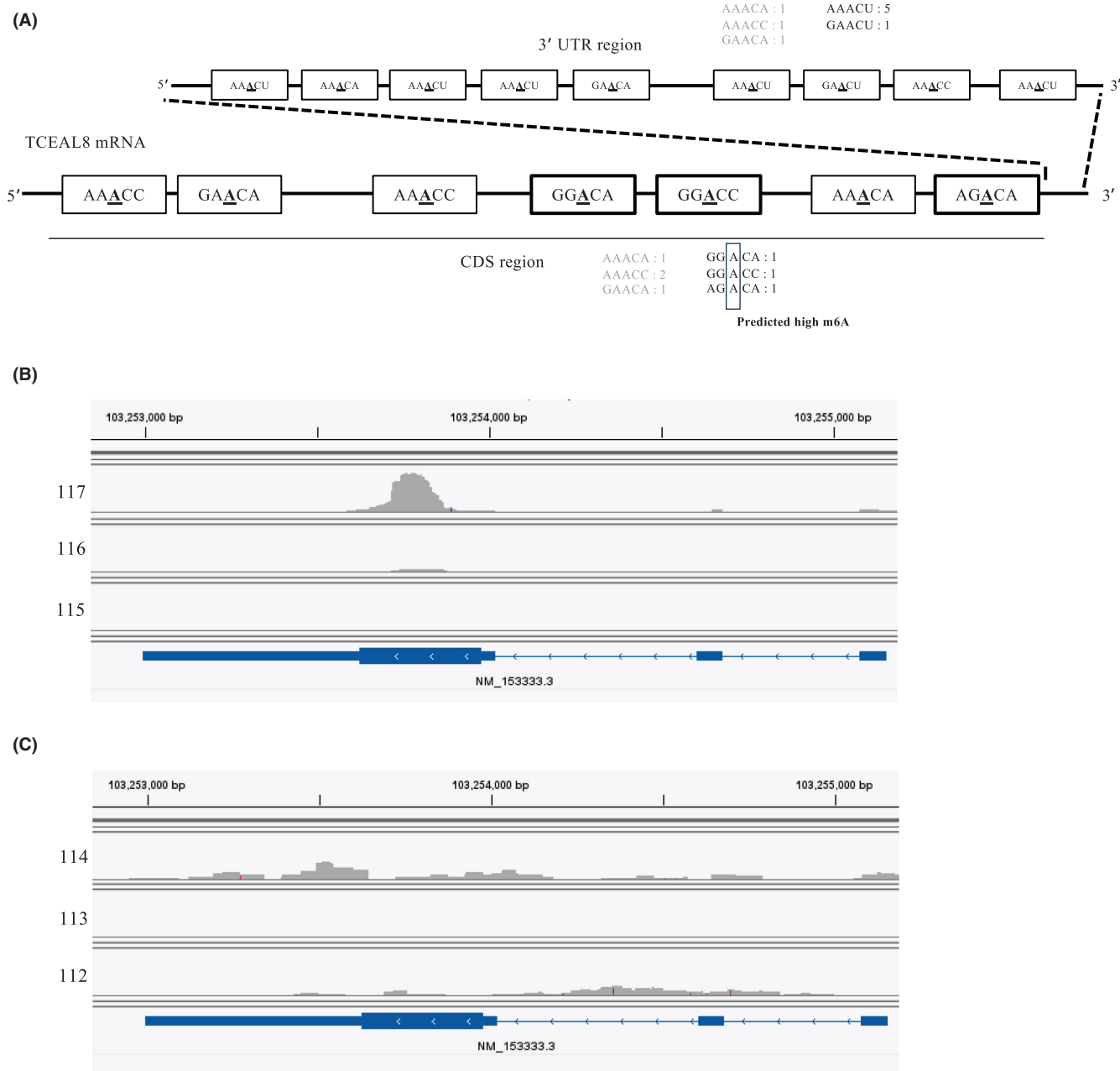


FIGURE 3 Mapping data obtained by methylated RNA immunoprecipitation sequencing (MeRIP-seq) to the TCEAL8 gene. (A) RRACH (R: A or G, H: A, T, or C) sequences in TCEAL8 mRNA. The total number of each RRACH in the CDS region or 3' UTR region was counted. The middle A in GGACA, GGACC and AGACA of CDS region was predicted high m6A. (B) Mapping results of 117 cancer tissues, 116 duct tissues, and 115 acinar tissues obtained by MeRIP-seq to the TCEAL8 gene. Max on the vertical axis is 400 counts. (C) Mapping results of MeRIP-seq-derived 114 cancer tissues, 113 duct tissues, and 112 acinar tissues to the TCEAL8 gene. Max of vertical axis is 50 counts.

reanalyzed. As shown in Figure 4B, cancer-associated pathways were detected (Figure S6A). To examine the function of m6A-activated TCEAL8 mRNA, we examined METTL3 expression. METTL3 was found to be expressed in 1358 spots, and METTL3-positive cells were as widely distributed as TCEAL8 (Figure 4C). TCEAL8-positive and METTL3-positive cells were found in 198 spots (Figure 4D, Table S1). Among them, 85 spots were highly expressing TCEAL8 and METTL3 (Figure S6B). Since METTL3-positive spots were presumed to have more highly m6A-modified RNA, we compared gene expression in TCEAL8-positive METTL3-positive and TCEAL8-positive

METTL3-negative spots by GSEA. The results showed activation of Notch and mTOR signaling in TCEAL8-positive METTL3-positive spots (Figure 4E). These signaling pathways have been reported to promote cancer invasion and metastasis,^{26,27} suggesting that m6A-activated TCEAL8 mRNA promotes cancer malignancy. In GSEA of high- and low-TCEAL8-expression spots in METTL3-positive spots, the high-TCEAL8-expression spots showed increased expression of ribosomal genes, p53 signaling pathway, JAK-STAT signaling pathway, and pancreatic cancer-related genes (Figure S7). Grouping of each spot by t-SNE plots resulted in four groups (Figure S8A). TCEAL8 was

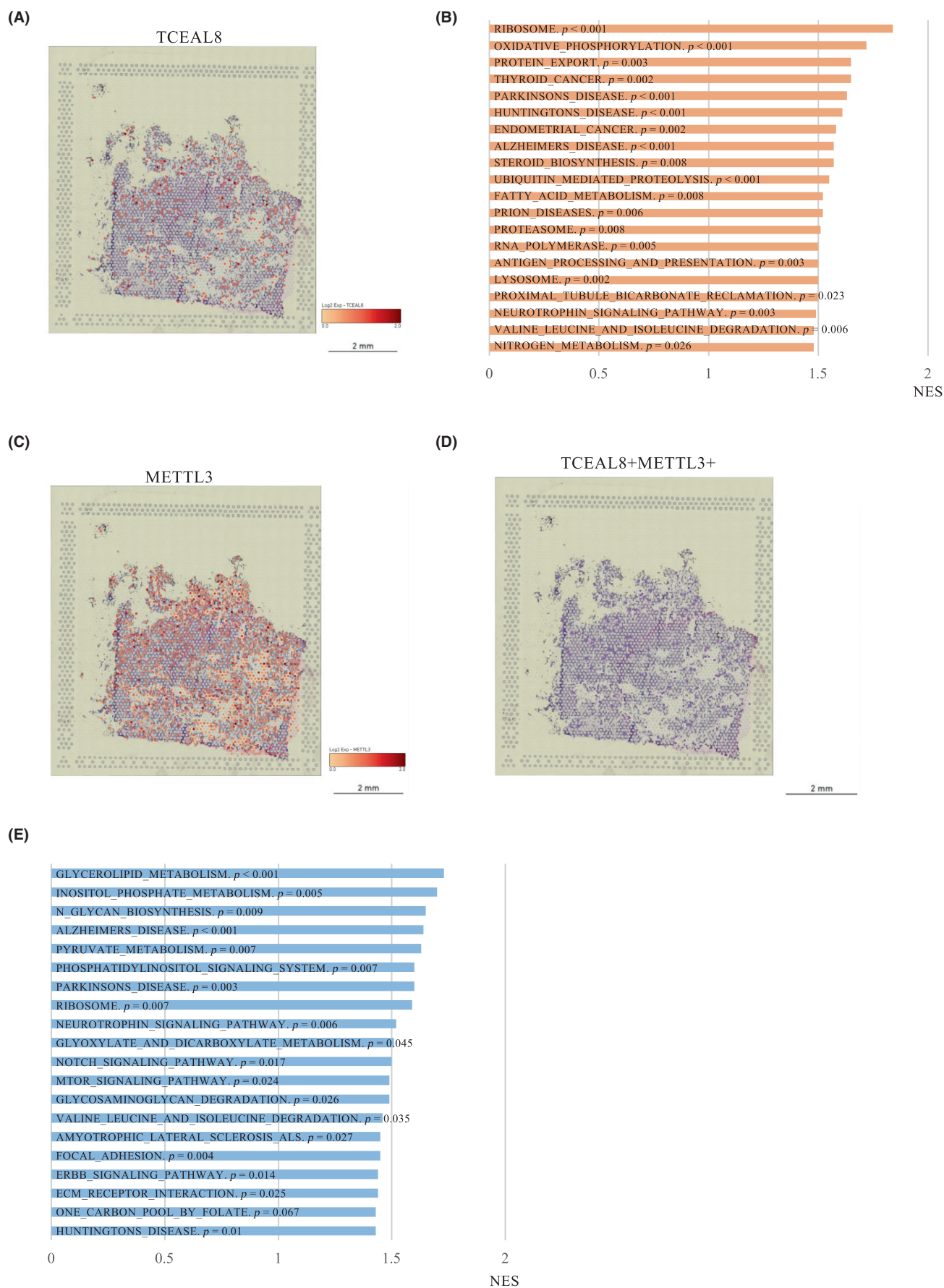


FIGURE 4 Spatially resolved transcriptomic results of cancer tissue. (A) TCEAL8 expression results for each spot. (B) Results of GSEA with KEGG pathway for TCEAL8-positive cells against TCEAL8-negative spots. Horizontal axis is normalized enrichment score (NES). (C) Expression of METTL3 in each spot. (D) TCEAL8-positive and METTL3-positive spots. (E) Results of GSEA with KEGG pathway performed on TCEAL8-positive and METTL3-positive spots compared with TCEAL8-positive and METTL3-negative spots. Horizontal axis is NES.

expressed in many spots in clusters 1 and 2 (Figure S8B). Gene expression analysis of each cluster showed that OLFM4 had a similar expression distribution as TCEAL8, suggesting that TCEAL8 is involved in the expression of OLFM4 (Figure S8C).

4 | DISCUSSION

In this study, gene expression and m6A-modified genes in pancreatic cancer clinical samples and normal tissue cells were examined by MeRIP-seq to identify m6A-activated pancreatic cancer marker RNAs. Among them, TCEAL8, a member of the transcription elongation factor-like protein family, is a functionally unknown gene that has rarely been reported. The three-dimensional structure of TCEAL8 has not been analyzed, but the structure has been predicted by the AlphaFold Protein Structure Database. GSEA of spatially resolved transcriptomic data (TCEAL8+ vs. TCEAL8-) in cancer showed that ribosomal proteins were the primary activation pathway in both cases, suggesting that the basic function of TCEAL8 is to express ribosomal proteins (Figure 4B).

Cancer-related signals were activated when TCEAL8 was expressed in cancer tissues (Figure 4B) and in cancer tissues expressing m6A-activated TCEAL8 mRNA (Figure 4E). These results suggest that TCEAL8 expression and m6A-modified TCEAL8 mRNA expression in pancreatic cancer tissues do not act in an inhibitory manner on pancreatic cancer growth. TCEAL8 may be involved in the transcription of genes detected in the cancer-related pathway. TCEAL8 expression was upregulated by m6A modification. The expression level of TCEAL8 was increased by m6A modification. This suggests that m6A modification stabilizes TCEAL8 mRNA. MeRIP-seq revealed that the CDS region of TCEAL8 is particularly m6A modified. By comparing the 3' UTR sequence with the CDS sequence, we identified three highly m6A-modified METTL3-binding sequences. This suggests that such sequences are highly m6A modified by METTL3 in pancreatic cancer.

According to The Human Protein Atlas database, high and low expression of TCEAL8 in cancer patients has been associated with altered prognosis (Figure S9). The ChIP-Atlas database also showed acetylation of histone H3K27, an open chromatin marker, in the transcription start region of TCEAL8 in pancreatic cancer cells (Figure S10). Mutations in E19V (KM12), P66H (SNU1040), and P110N (HCC1359) and fusion of BPTF-TCEAL8 (UBLC1) have been reported in the DepMap database. Therefore, TCEAL8 may affect cancer cell proliferation. Visium analysis showed that TCEAL8 has a similar expression distribution to OLFM4. OLFM4 has been reported to be associated with drug resistance and poor prognosis in pancreatic cancer.²⁸ It has been reported that Notch signaling in intestinal epithelium cells promotes the expression of OLFM4 and

contributes to its cytoprotective effects.²⁹ Therefore, TCEAL8 might be involved in such effects. In the pancreatic cancer tissues in which MeRIP-seq was performed in this study, there was an increase in m6A-activated TCEAL8 mRNA in all samples compared with duct in the same patients. Since the pancreatic cancers used in this study are early-stage pancreatic cancers that can be surgically resected, routine quantification of m6A-activated TCEAL8 mRNA may be useful in the detection of early-stage pancreatic cancer.

This study shows for the first time that m6A-activated TCEAL8 mRNA is a potential pancreatic cancer tissue marker and that TCEAL8 may be involved in pancreatic cancer growth. A variety of cancer-promoting and tumor-suppressive miRNAs have been reported in cancer.³⁰ Therefore, miRNAs targeting TCEAL8 may be applicable to pancreatic cancer therapy as cancer suppressor genes. Further studies are needed to determine which genes are directly involved in the expression of TCEAL8 as a transcriptional elongation factor.

AUTHOR CONTRIBUTIONS

Tomoaki Hara: Conceptualization; data curation; formal analysis; investigation; methodology; resources; software; validation; visualization; writing – original draft; writing – review and editing. **Sikun Meng:** Conceptualization; data curation; formal analysis; investigation; methodology; project administration; resources; software; validation; visualization; writing – original draft; writing – review and editing. **Hiromichi Sato:** Methodology; resources; software; validation; visualization; writing – original draft; writing – review and editing. **Shotaro Tatekawa:** Resources; software; validation; visualization. **Kazuki Sasaki:** Resources; software; validation; visualization. **Yu Takeda:** Resources; validation; visualization. **Yoshiko Tsuji:** Investigation; methodology. **Yasuko Arai:** Investigation; methodology. **Ken Ofusa:** Conceptualization; formal analysis; investigation; methodology; software; validation; writing – original draft. **Toru Kitagawa:** Conceptualization; investigation; project administration; resources; supervision. **Daisaku Yamada:** Resources; supervision; validation; visualization. **Hidenori Takahashi:** Resources; supervision; validation; visualization. **Shogo Kobayashi:** Resources; supervision; validation. **Daisuke Motooka:** Data curation; formal analysis; investigation; methodology; software; validation; visualization. **Yutaka Suzuki:** Data curation; methodology; resources; software; supervision. **Sarah Rennie:** Data curation; formal analysis; investigation; methodology; software; supervision; visualization; writing – original draft. **Shizuka Uchida:** Conceptualization; data curation; investigation; methodology; project administration; software; supervision. **Masaki Mori:** Conceptualization; project administration; supervision. **Kazuhiko Ogawa:** Conceptualization; investigation; supervision. **Yuichiro Doki:** Conceptualization; supervision. **Hidetoshi Eguchi:** Project administration; supervision; validation. **Hideshi Ishii:** Conceptualization; data curation; formal analysis;

funding acquisition; investigation; methodology; project administration; supervision; validation; visualization; writing – original draft; writing – review and editing.

ACKNOWLEDGMENTS

The authors are grateful to all the lab members. The authors thank the Department of Gastroenterological Surgery, Osaka University Graduate School of Medicine for providing surgical samples and the University of Tokyo Center for Frontier Sciences, one of the Integrated Information Analysis Groups of the Platform for Advanced Genome Science, for RNA-seq analysis.

FUNDING INFORMATION

This work was supported in part by a Grant-in-Aid for Scientific Research from the Ministry of Education, Culture, Sports, Science and Technology (17cm0106414h0002; JP21lm0203007; JP23ym0126809; 19K22658; 20H00541; 21K19526; 22H03146; 22K19559; 23K18313; 16H06279 [PAGS]). Partial support was offered by the Mitsubishi Foundation (2021-48) and Takahashi Industrial and Economic Research Foundation (2023) to H.I.

CONFLICT OF INTEREST STATEMENT

Partial institutional endowments were received from Hirotu Bio Science Inc. (Tokyo, Japan), Kinshu-kai Medical Corporation (Osaka, Japan), Kyowa-kai Medical Corporation (Osaka, Japan), IDEA Consultants Inc. (Tokyo, Japan), and Unitech Co. Ltd. (Chiba, Japan). Ke.O. is an employee of IDEA Consultants Inc. (Tokyo, Japan). T.K. is a CEO of Kyowa-kai Medical Corporation (Osaka, Japan). Ka.O., Y.D., H.E., and H.I. are associate editors of this journal. Others have no conflict of interest for this study.

DATA AVAILABILITY STATEMENT

MeRIP-Seq analysis data were reviewed and approved by the NBDC Human Data Review Committee. Data were registered with the NBDC Human Database (hum0421).

ETHICS STATEMENT

Approval of the research protocol by an Institutional Reviewer Board: This study was approved by the Research Ethics Committee of Osaka University (approval no. 21181).

Informed Consent: Written informed consent was obtained from the patients.

Registry and the Registration No. of the study/trial: MeRNA-seq data were registered with the NBDC Human Database (hum0421).

Animal Studies: N/A.

ORCID

Yu Takeda  <https://orcid.org/0000-0001-7210-5096>

Daisaku Yamada  <https://orcid.org/0000-0002-6702-3800>

Hidehiko Takahashi  <https://orcid.org/0000-0003-4801-3540>

Hidetoshi Eguchi  <https://orcid.org/0000-0002-2318-1129>

Hideshi Ishii  <https://orcid.org/0000-0002-0632-6517>

REFERENCES

- Zhou Z, Lv J, Yu H, et al. Mechanism of RNA modification N6-methyladenosine in human cancer. *Mol Cancer*. 2020;19:104. doi:[10.1186/s12943-020-01216-3](https://doi.org/10.1186/s12943-020-01216-3)
- Lei K, Lin S, Yuan Q. N6-methyladenosine (m6A) modification of ribosomal RNAs (rRNAs): critical roles in mRNA translation and diseases. *Genes Dis*. 2021;10:126-134. doi:[10.1016/j.gendis.2021.10.005](https://doi.org/10.1016/j.gendis.2021.10.005)
- Ruszkowska A. METTL16, methyltransferase-like protein 16: current insights into structure and function. *Int J Mol Sci*. 2021;22:2176. doi:[10.3390/ijms22042176](https://doi.org/10.3390/ijms22042176)
- Qi YN, Liu Z, Hong LL, Li P, Ling ZQ. Methyltransferase-like proteins in cancer biology and potential therapeutic targeting. *J Hematol Oncol*. 2023;16:89. doi:[10.1186/s13045-023-01477-7](https://doi.org/10.1186/s13045-023-01477-7)
- Imanishi M. Mechanisms and strategies for determining m6A RNA modification sites by natural and engineered m6A effector proteins. *Chem Asian J*. 2022;17:e202200367. doi:[10.1002/asia.202200367](https://doi.org/10.1002/asia.202200367)
- Deng X, Qing Y, Horne D, Huang H, Chen J. The roles and implications of RNA m6A modification in cancer. *Nat Rev Clin Oncol*. 2023;20:507-526. doi:[10.1038/s41571-023-00774-x](https://doi.org/10.1038/s41571-023-00774-x)
- Sendinc E, Shi Y. RNA m6A methylation across the transcriptome. *Mol Cell*. 2023;83:428-441. doi:[10.1016/j.molcel.2023.01.006](https://doi.org/10.1016/j.molcel.2023.01.006)
- Flamand MN, Tegowski M, Meyer KD. The proteins of mRNA modification: writers, readers, and erasers. *Annu Rev Biochem*. 2023;92:145-173. doi:[10.1146/annurev-biochem-052521-035330](https://doi.org/10.1146/annurev-biochem-052521-035330)
- Dominissini D, Moshitch-Moshkovitz S, Schwartz S, et al. Topology of the human and mouse m6A RNA methylomes revealed by m6A-seq. *Nature*. 2012;485:201-206. doi:[10.1038/nature11112](https://doi.org/10.1038/nature11112)
- Tsuiji Y, Hara T, Meng S, et al. Role of RNA methylation in the regulation of pancreatic cancer stem cells (Review). *Oncol Lett*. 2023;26:336. doi:[10.3892/ol.2023.13922](https://doi.org/10.3892/ol.2023.13922)
- Panneerdoss S, Eedunuri VK, Yadav P, et al. Cross-talk among writers, readers, and erasers of m6A regulates cancer growth and progression. *Sci Adv*. 2018;4:eaar8263. doi:[10.1126/sciadv.aar8263](https://doi.org/10.1126/sciadv.aar8263)
- Lee JH, Hong J, Zhang Z, et al. Regulation of telomere homeostasis and genomic stability in cancer by N6-adenosine methylation (m6A). *Sci Adv*. 2021;7:eabg7073. doi:[10.1126/sciadv.abg7073](https://doi.org/10.1126/sciadv.abg7073)
- Tatekawa S, Tamari K, Chijimatsu R, et al. N(6)-methyladenosine methylation-regulated polo-like kinase 1 cell cycle homeostasis as a potential target of radiotherapy in pancreatic adenocarcinoma. *Sci Rep*. 2022;12:11074. doi:[10.1038/s41598-022-15196-5](https://doi.org/10.1038/s41598-022-15196-5)
- Zhang S, Lai T, Su X, et al. Linc00662 m6A promotes the progression and metastasis of pancreatic cancer by activating focal adhesion through the GTF2B-ITGA1-FAK pathway. *Am J Cancer Res*. 2023;13:1718-1743.
- Lu J, Yu L, Xie N, Wu Y, Li B. METTL14 facilitates the metastasis of pancreatic carcinoma by stabilizing LINC00941 in an m6A-IGF2BP2-dependent manner. *J Cancer*. 2023;14:1117-1131. doi:[10.7150/jca.84070](https://doi.org/10.7150/jca.84070)
- Chen S, Zhou Y, Chen Y, Gu J. fastp: an ultra-fast all-in-one FASTQ preprocessor. *Bioinformatics*. 2018;34:i884-i890. doi:[10.1093/bioinformatics/bty560](https://doi.org/10.1093/bioinformatics/bty560)
- Langmead B, Salzberg SL. Fast gapped-read alignment with Bowtie 2. *Nat Methods*. 2012;9:357-359. doi:[10.1038/nmeth.1923](https://doi.org/10.1038/nmeth.1923)
- Dobin A, Davis CA, Schlesinger F, et al. STAR: ultrafast universal RNA-seq aligner. *Bioinformatics*. 2013;29:15-21. doi:[10.1093/bioinformatics/bts635](https://doi.org/10.1093/bioinformatics/bts635)
- Robinson JT, Thorvaldsdóttir H, Winckler W, et al. Integrative genomics viewer. *Nat Biotechnol*. 2011;29:24-26. doi:[10.1038/nbt.1754](https://doi.org/10.1038/nbt.1754)
- Ge SX, Son EW, Yao R. iDEP: an integrated web application for differential expression and pathway analysis of RNA-Seq data. *BMC Bioinformatics*. 2018;19:534. doi:[10.1186/s12859-018-2486-6](https://doi.org/10.1186/s12859-018-2486-6)

21. Torre D, Lachmann A, Ma'ayan A. BioJupies: automated generation of interactive notebooks for RNA-Seq data analysis in the cloud. *Cell Syst*. 2018;7:556-561.e3. doi:[10.1016/j.cels.2018.10.007](https://doi.org/10.1016/j.cels.2018.10.007)
22. Ogata H, Goto S, Sato K, Fujibuchi W, Bono H, Kanehisa M. KEGG: Kyoto Encyclopedia of Genes and Genomes. *Nucleic Acids Res*. 1999;27:29-34. doi:[10.1093/nar/27.1.29](https://doi.org/10.1093/nar/27.1.29)
23. Subramanian A, Tamayo P, Mootha VK, et al. Gene set enrichment analysis: a knowledge-based approach for interpreting genome-wide expression profiles. *Proc Natl Acad Sci USA*. 2005;102:15545-15550. doi:[10.1073/pnas.0506580102](https://doi.org/10.1073/pnas.0506580102)
24. Chijimatsu R, Kobayashi S, Takeda Y, et al. Establishment of a reference single-cell RNA sequencing dataset for human pancreatic adenocarcinoma. *iScience*. 2022;25:104659. doi:[10.1016/j.isci.2022.104659](https://doi.org/10.1016/j.isci.2022.104659)
25. Satija R, Farrell JA, Gennert D, Schier AF, Regev A. Spatial reconstruction of single-cell gene expression data. *Nat Biotechnol*. 2015;33:495-502. doi:[10.1038/nbt.3192](https://doi.org/10.1038/nbt.3192)
26. Han S, Cao C, Liu R, et al. GAS41 mediates proliferation and GEM chemoresistance via H2A.Z.2 and Notch1 in pancreatic cancer. *Cell Oncol (Dordr)*. 2022;45:429-446. doi:[10.1007/s13402-022-00675-8](https://doi.org/10.1007/s13402-022-00675-8)
27. Qin T, Xiao Y, Qian W, et al. HGF/c-Met pathway facilitates the perineural invasion of pancreatic cancer by activating the mTOR/NGF axis. *Cell Death Dis*. 2022;13:387. doi:[10.1038/s41419-022-04799-5](https://doi.org/10.1038/s41419-022-04799-5)
28. Ohkuma R, Yada E, Ishikawa S, et al. High expression of olfactomedin-4 is correlated with chemoresistance and poor prognosis in pancreatic cancer. *PLoS One*. 2020;15:e0226707. doi:[10.1371/journal.pone.0226707](https://doi.org/10.1371/journal.pone.0226707)
29. Kuno R, Ito G, Kawamoto A, et al. Notch and TNF- α signaling promote cytoplasmic accumulation of OLFM4 in intestinal epithelium cells and exhibit a cell protective role in the inflamed mucosa of IBD patients. *Biochem Biophys Res*. 2021;25:100906. doi:[10.1016/j.bbrep.2020.100906](https://doi.org/10.1016/j.bbrep.2020.100906)
30. Sato H, Hara T, Meng S, et al. Drug discovery and development of miRNA-based nucleotide drugs for gastrointestinal cancer. *Biomedicine*. 2023;11:2235. doi:[10.3390/biomedicines11082235](https://doi.org/10.3390/biomedicines11082235)

SUPPORTING INFORMATION

Additional supporting information can be found online in the Supporting Information section at the end of this article.

How to cite this article: Hara T, Meng S, Sato H, et al. High N6-methyladenosine-activated TCEAL8 mRNA is a novel pancreatic cancer marker. *Cancer Sci*. 2024;00:1-11. doi:[10.1111/cas.16152](https://doi.org/10.1111/cas.16152)